iScience

CellPress
OPEN ACCESS

Article

# Unraveling cartilage degeneration through synergistic effects of hydrostatic pressure and biomimetic temperature increase

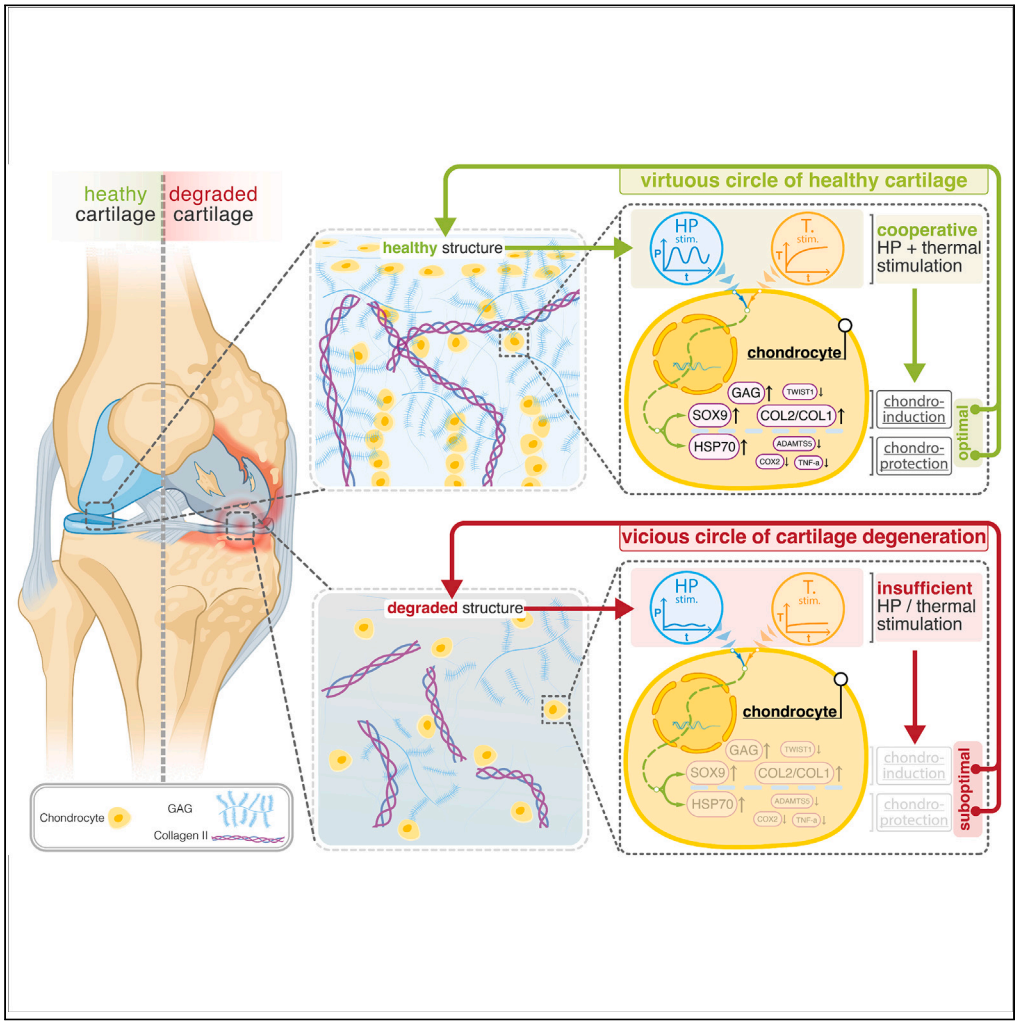


Yanheng Guo, Theofanis Stampoultzis, Naser Nasrollahzadeh, Peyman Karami, Vijay Kumar Rana, Lee Applegate, Dominique P. Pioletti

dominique.pioletti@epfl.ch

## Highlights

Development of novel dual-biophysical HP-T bioreactor system

HP-T synergistically affects chondro-induction/-protection in human chondrocytes

HP enhanced chondrocyte sensitivity to thermal stimulation

Suggested new theory on the cartilage homeostasis and vicious cycle

Guo et al., iScience 26, 108519
December 15, 2023 
https://doi.org/10.1016/j.isci.2023.108519

iScience

CellPress
OPEN ACCESS

Article

# Unraveling cartilage degeneration through synergistic effects of hydrostatic pressure and biomimetic temperature increase

Yanheng Guo,[1,3] Theofanis Stampoultzis,[1,3] Naser Nasrollahzadeh,[1] Peyman Karami,[1] Vijay Kumar Rana,[1] Lee Applegate,[2] and Dominique P. Pioletti[1,4,*]

## SUMMARY

**Cartilage degeneration, typically viewed as an irreversible, vicious cycle, sees a significant reduction in two essential biophysical cues: the well-established hydrostatic pressure (HP) and the recently discovered transient temperature increase. Our study aimed to evaluate the combined influence of these cues on maintaining cartilage homeostasis. To achieve this, we developed a customized bioreactor, designed to mimic the specific hydrostatic pressure and transient thermal increase experienced during human knee physiological activities. This system enabled us to investigate the response of human 3D-cultured chondrocytes and human cartilage explants to either isolated or combined hydrostatic pressure and thermal stimuli. Our study found that chondroinduction (SOX9, aggrecan, and sulfated glycosaminoglycan) and chondroprotection (HSP70) reached maximum expression levels when hydrostatic pressure and transient thermal increase acted in tandem, underscoring the critical role of these combined cues in preserving cartilage homeostasis. These findings led us to propose a refined model of the vicious cycle of cartilage degeneration.**

## INTRODUCTION

Degenerated cartilage represents a state of disequilibrium, where chondrocytes struggle to synthesize sufficient extracellular matrix and cope with the burdens of oxidative and biomechanical stress. This disturbance of homeostasis in turn catalyzes the further progression of a variety of pathological conditions like osteoarthritis (OA) resulting in a vicious circle of cartilage degeneration (Figure 1A).[1–3] To date, numerous studies have investigated the progression of cartilage degeneration from various perspectives such as inflammatory cytokines,[4,5] oxidative stress,[6,7] catabolic signaling pathways,[8] and mechanotransduction.[9] In this article, we adopt an original perspective to further extend our knowledge of the vicious circle of the cartilage degeneration. Having observed that two naturally coupled biophysical signals, dynamic hydrostatic pressure (HP) and thermal stimulation, are greatly diminished in deteriorated cartilage, we are motivated to explore their significance in perpetuating the vicious circle.[10–13]

During daily activities like walking or running, healthy joints experience compressive cyclic loading. Chondrocytes within loaded tissue perceive three major mechanical effects: compressive strain, shear stress, and hydrostatic pressure (HP).[10] Concurrently, secondary effects such as transient temperature increases also arise as byproducts of mechanical load.[12,14] Hyaline cartilage has been shown to dissipate part of mechanical strain energy through heat production, a phenomenon known as self-heating.[12] Therefore, HP and thermal stimulation coexist as byproducts of cyclic compressive loading in healthy cartilage. Osteoarthritis alters the cartilage tissue's microstructure, causing a significant decrease in the magnitude of these two physiological stimulations. Among the different sources of heat contributing to the observed thermal increase in healthy cartilage, the temperature rise induced by energy dissipation is considered to be a major heat source. However, in degenerated cartilage, the impaired ability to dissipate energy, resulting from the loss of essential extracellular matrix (ECM) components, notably reduces the amount of heat generated during repetitive loading.[12] Moreover, due to lower glycosaminoglycan (GAG) content, higher porosity and permeability, degenerated cartilage generates much lower HP stimulation during cyclic loading compared to healthy tissue.[13,15]

Previous research has demonstrated some beneficial effects of isolated HP and thermal stimulations on chondrocytes. *In vitro* bioreactor studies revealed that physiological-range HP stimulation can increase chondrogenic markers like SRY-box transcription factor 9 (SOX9), stimulate extracellular matrix formation (aggrecan (ACAN) and collagen type II (COL2a)), and regulate oxidative stress related to OA pathogenesis in stem cells or chondrocytes.[16] Additionally, culture temperature plays a crucial role in chondrocyte metabolic activity.[17,18] Studies have

[1]Laboratory of Biomechanical Orthopedics, Institute of Bioengineering, EPFL, Lausanne, Switzerland
[2]Regenerative Therapy Unit, Lausanne University Hospital, University of Lausanne, Lausanne, Switzerland
[3]These authors contributed equally
[4]Lead contact
*Correspondence: dominique.pioletti@epfl.ch
https://doi.org/10.1016/j.isci.2023.108519

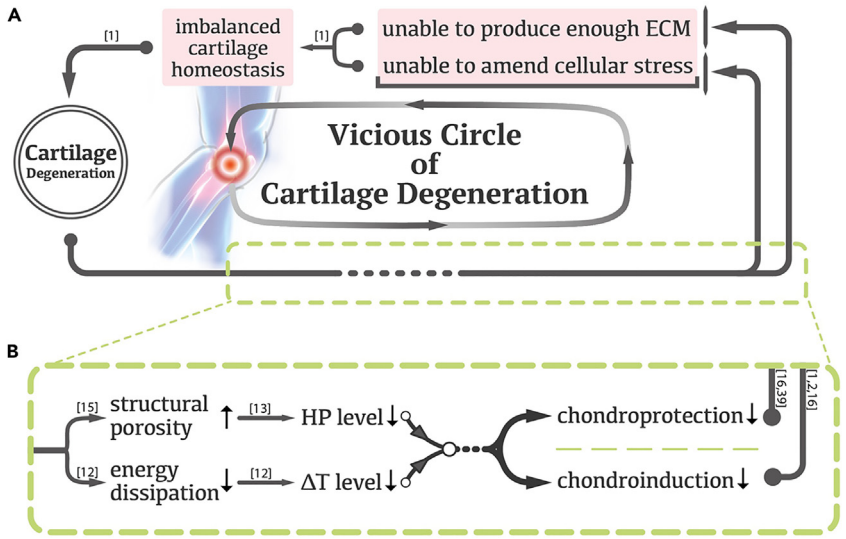


**Figure 1. The conventional vicious circle of cartilage degeneration**

(A) Conventional version and (B) a more elaborated version based on existing literatures (presented in []) and new findings from this study focusing on the cooperative role of hydrostatic pressure (illustrated as "HP") and biomimetic thermal stimulation (illustrated as "ΔT").

shown that chondrocytes express more chondrogenic markers when exposed to temperature increases similar to those experienced during repetitive physiological activities, compared to samples incubated at a steady 37°C (core body temperature) or 32.5°C (resting knee temperature).[19,20] Thermomechanical stimulation, combining compression loading with a temperature increase, yielded a synergistic impact on chondrogenic marker expression in chondroprogenitor-seeded constructs. Despite the potential significance, previous research has predominantly focused on the effects of isolated stimulation forms, neglecting the possible interactions between them. Motivated by these findings, we hypothesize that an insufficient cooperation of the two essential byproducts of compressive loading (i.e., HP and thermal stimulation) in degenerated cartilage might exacerbate the cartilage deterioration. Consequently, in this article, we sought to evaluate the effect of the cooperative stimulation of hydrostatic pressure and biomimetic thermal increase on maintaining cartilage homeostasis from two complementary perspectives: chondroinduction and chondroprotection.

Herein, we embarked on a comprehensive series of studies to investigate the function of HP and biomimetic thermal stimulations with the perspective to further understand how the establishment of a vicious circle can lead to irreversible cartilage degeneration. Toward achieving such an objective, we first developed a new bioreactor system capable of recapitulating the profile of pressure and temperature present in healthy knee cartilage tissue upon cyclic loading. We then encapsulated primary human chondrocytes in gelatin-methacryloyl (GelMA) hydrogels. Cell-laden constructs were subsequently subjected to isolated or combined forms of stimulation (Figure 2). To assess chondroinductive and chondroprotective behavior, we examined gene and protein expression and performed immunofluorescent analyses to explore the changes of important regulators of chondrogenesis and critical components involved in maintaining chondrocyte homeostasis. Human cartilage explants were also employed in this research to corroborate the findings to a certain degree. To conclude the study, we proposed a new understanding on the irreversibility of cartilage degeneration through an expanded version of the vicious circle as depicted in Figure 1B. Here, we placed a new focus on the cooperative effect of HP and biomimetic thermal stimulation on the chondroinduction and chondroprotection behavior of chondrocytes and its implication in sustaining the vicious circle.

## RESULTS

### Development of bioreactor system for hydrostatic pressure and thermal stimulation

In our pursuit to examine the cooperative effects of hydrostatic pressure (HP) and biomimetic thermal increase—byproducts of repetitive compressive loadings—on chondrocyte homeostasis, a bioreactor enabling the application of these stimuli both individually and in combination to biological constructs became indispensable. However, the specific nature of HP rendered our previously used compression bioreactor, despite its temperature modulation capability, unsuitable for this investigation.[19] Consequently, to overcome this challenge and test our hypothesis, we devised a customized bioreactor system proficient in delivering isolated or combined forms of HP and thermal stimulation to cell-laden structures (Figure 3).

Hydrostatic pressure was delivered into the HP-thermal (HP-T) bioreactor by means of a hydraulic system driven by the linear actuator of an Electropuls dynamic test system, which was compressed against a metal syringe. The syringe was then connected via HPLC tubing to six loading chambers through a manifold. Swagelok tube fittings were used to secure the leak-free connection between the tubing and the customized HP loading chambers. We designed an interlocking self-sealing (ILSS) unit for the chamber's sealing system. The ILSS unit,

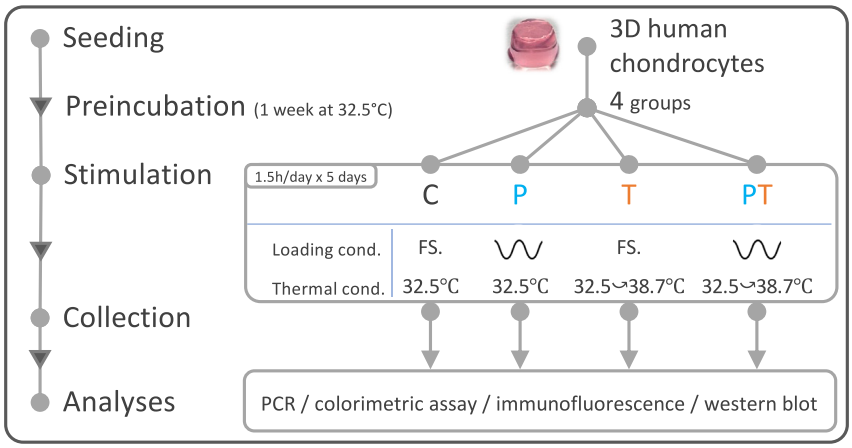


**Figure 2. Experimental design of HP-thermal stimulation study**

comprising a rotationally fixed metal ring positioned between an O-ring and a polydimethylsiloxane (PDMS) membrane, serves a dual purpose: it ensures physical separation between the sterile and non-sterile parts of the system and prevents leakage from the loading unit, even under maximal physiological pressure (up to 10 MPa). The leak-free property of the ILSS design under high hydrostatic pressure was also validated using COMSOL Multiphysics. To monitor the pressure inside the HP system, a piezoresistive pressure transmitter was connected to one of the loading chambers. The transmitter communicates with a microprocessor which is sequentially connected to a computer through serial communication where the real-time pressure is plotted using a customized MATLAB interface. Similarly, a thermal sensor was incorporated into one of the chambers to complete the feedback loop for the PID algorithm of the heating platform so that a controlled temperature increase can be obtained in the loading chamber following the predefined profile from 32.5°C to 38.7°C as described in our previous work.[19] We performed immunostaining on chondrocyte-laden constructs prior to subjecting them to stimulations. The imaging revealed functional biological samples expressing ACAN and the TRPV4 thermo-mechanosensing ion channel, indicative of their readiness for subsequent biophysical stimulations.

## Combined application of HP and thermal stimulation is necessary to maximize chondroinductive response in human chondrocytes

To investigate the chondroinductive response to various stimuli, we first utilized hydrogel constructs laden with adult primary human chondrocytes to examine the impact on two critical mediators of chondrogenesis: SOX9, the master regulator of chondrogenesis, and TWIST1, an inhibitor of SOX9 and chondrogenesis. HP stimulation alone did not significantly upregulate *SOX9* gene expression, while a 30% increase was achieved with isolated heat stimulation. Combined HP and thermal stimulation yielded the highest *SOX9* mRNA expression, 40% greater than the control group (Figure 4A). *TWIST1* expression decreased in groups receiving independent HP and thermal stimulation, with the lowest level observed when combined (35% reduction compared to control). Considering the antagonistic nature of SOX9 and TWIST1, we compared their expression ratios to evaluate the overall chondroinductive response (Figure 4B). The highest *SOX9*/*TWIST1* ratio was observed in samples exposed to cooperative biophysical stimuli. The absence of either thermal or HP stimulation significantly diminished this effect. A similar trend was observed when using primary human chondrocytes sourced from an infant (Figure S1). Immunofluorescent staining validated SOX9 and TWIST1 protein expression (Figure S2). Thermal stimulation alone increased SOX9 protein-positive cells, further amplified with HP stimulation (Figure 4C). TWIST1 protein-positive cells decreased in isolated HP and thermal stimulation, with the lowest percentage observed when combined (Figure 4D).

We then sought to focus on functional structural proteins in the downstream portion of chondrogenic signaling pathways. The gene expression ratio of collagen type II (*COL2A*) and collagen type I (*COL1A*) was analyzed. Isolated HP stimulation decreased the *COL2A*/*COL1A* ratio, but it was restored or enhanced with combined stimulation (Figures 4E and S3). Immunostaining targeting COL2A proteins was also conducted with no significant difference observed among groups. Aggrecan (*ACAN*) mRNA expression decreased with isolated HP stimulation but improved with combined HP and thermal stimulation (Figure 4F). This effect was subsequently confirmed at the protein level using immunofluorescence (Figure S4). *ADAMTS5*, an aggrecanase, was reduced in response to isolated HP or thermal stimulation and further decreased in samples subjected to cooperative stimulation. Colorimetric tests with DMMB were then used to assess chondrocytes' s-GAG production capacity (Figures 4G and S1). While not statistically significant, isolated HP and thermal stimulation slightly reduced average s-GAG production. However, combined stimulation substantially increased s-GAG production compared to controls or isolated stimulation. Our findings suggest a synergistic effect on chondroinductive response in 3D chondrocyte culture when HP and biomimetic thermal increase are applied simultaneously, as evidenced by increased expression of signaling regulators and critical structural proteins.

To further validate our hypothesis under more realistic conditions, human cartilage explants were collected and subjected to our innovative bioreactor's combined stimulation. Mass spectrometry analysis revealed an increase in specific collagen family proteins, notably COL2A

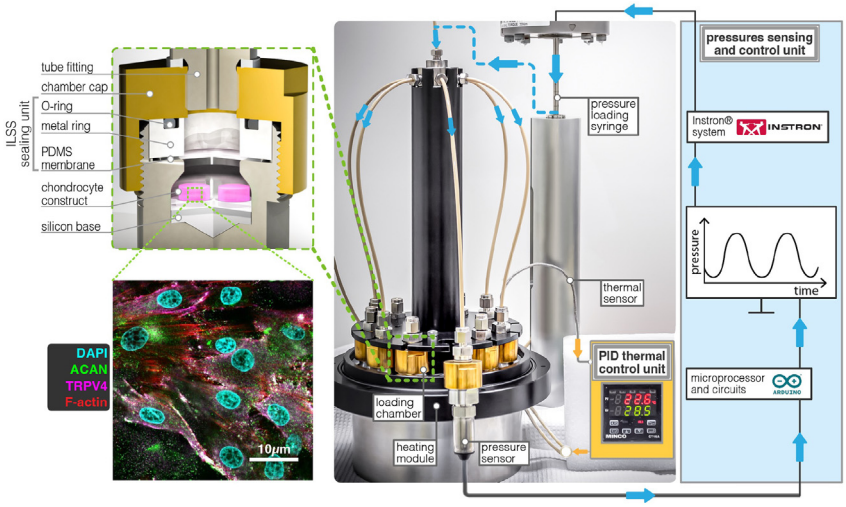


**Figure 3. Newly developed HP-T biophysical stimulation system with labels**

Blue and orange arrows denote the delivering chain of HP and temperature, respectively. Top-left insert shows the CAD design of the loading chamber, bottom-left insert shows immunofluorescent staining of the chondrocyte-laden GelMA construct after 7 days of preincubation.

and COL6, as well as other abundant structural proteins such as ACAN and cartilage oligomeric matrix protein (COMP), under the synergistic HP and thermal stimulation. The majority of matrix metallopeptidase (MMP) family members exhibited a decrease in response to the combined stimulation. Moreover, the lysyl oxidase family (LOX), which plays a crucial role in extracellular matrix stabilization and cartilage matrix formation, also demonstrated upregulation under the combined HP and thermal stimulation (Figure 4H). This evidence reinforces our hypothesis that the synergistic stimulation promotes enhanced chondroinduction.

## Cooperative HP and thermal stimulation enhanced chondroprotective effect in chondrocytes

For a better understanding of the vicious circle of cartilage deterioration from a chondroprotection standpoint, we examined the effect of HP and thermal stimulation on heat shock protein 70 (HSP70) in adult chondrocyte-laden constructs. HSP70 is a chaperone protein family that regulates various essential cellular processes such as protein folding and trafficking. Overexpression of HSP70 has been shown to protect chondrocytes from cellular injuries (either apoptotic or necrotic) and have protective effects on osteoarthritis (OA) cartilage.[21–24] First, gene expressions of the inducible isoform *HSP70I* and constitutive isoform *HSC70* were analyzed to capture the changes of the two essential members of HSP70 family (hereafter referred to as "HSP70s" when the two isoforms are not distinguished) (Figure 5A). While isolated form of HP stimulation did not raise *HSP70s*, applying heat stimulation alone increased *HSP70I* and *HSC70* gene expressions by 14- and 18-fold, respectively. Surprisingly, when HP and heat stimulations were combined, the gene expression levels of *HSP70s* increased by an additional 30% for *HSP70I* and 50% for *HSC70* compared to their counterparts after isolated thermal stimulation. Following this, immunoblotting was conducted to examine the changes at the protein level for both the HSP70 family and the inducible isoform HSP70I. A comparable trend to that of the genes was observed; however, the rise from isolated thermal stimulation to combined stimulation was not as pronounced as it was at their gene transcriptional level. (Figure 5B). To further visualize and validate the synergistic effect on HSP70, immunostaining was performed (Figure 5C) and quantified (Figure 5E). The fluorescent signal of HSP70 was enhanced when thermal stimulation was applied, and the effect was further amplified when combined with HP stimulation. The immunofluorescent staining of HSP70I was also conducted (Figure 5D) and quantified (Figure 5F). Comparable to the results obtained for HSP70, the peak values were also observed in the group subjected to combined stimulation. We broadened our analysis of HSP70 to encompass the entire HSP family and examined it in a more realistic context using human cartilage explants subjected to combined HP and thermal stimulation (Figure 5G). The majority of HSP family members, including HSP70I (represented as HSPA1) and HSC70 (represented as HSPA8), displayed upregulation to varying degrees following the combined stimulation.

In addition, cyclooxygenase 2 (*COX2*) and tumor necrosis factor alpha (*TNF-a*), whose suppressions have been shown to be beneficial against OA,[25–27] were also studied at the level of gene transcription. The expression levels reached to the lowest in the group when the combined form of stimulation was applied to the cell-laden construct (Figure S5).

## DISCUSSION

Over recent decades, significant efforts have focused on understanding cartilage degeneration mechanisms to develop effective OA treatments. Progress has been made by examining various factors, including inflammatory and catabolic mediators (e.g., NF-kB, IL-10, TNF-a, MMPs, and ADAMTS) and their related signaling pathways (e.g., MAPK pathways and p38 kinase cascade).[28] Oxidative stress's role in OA

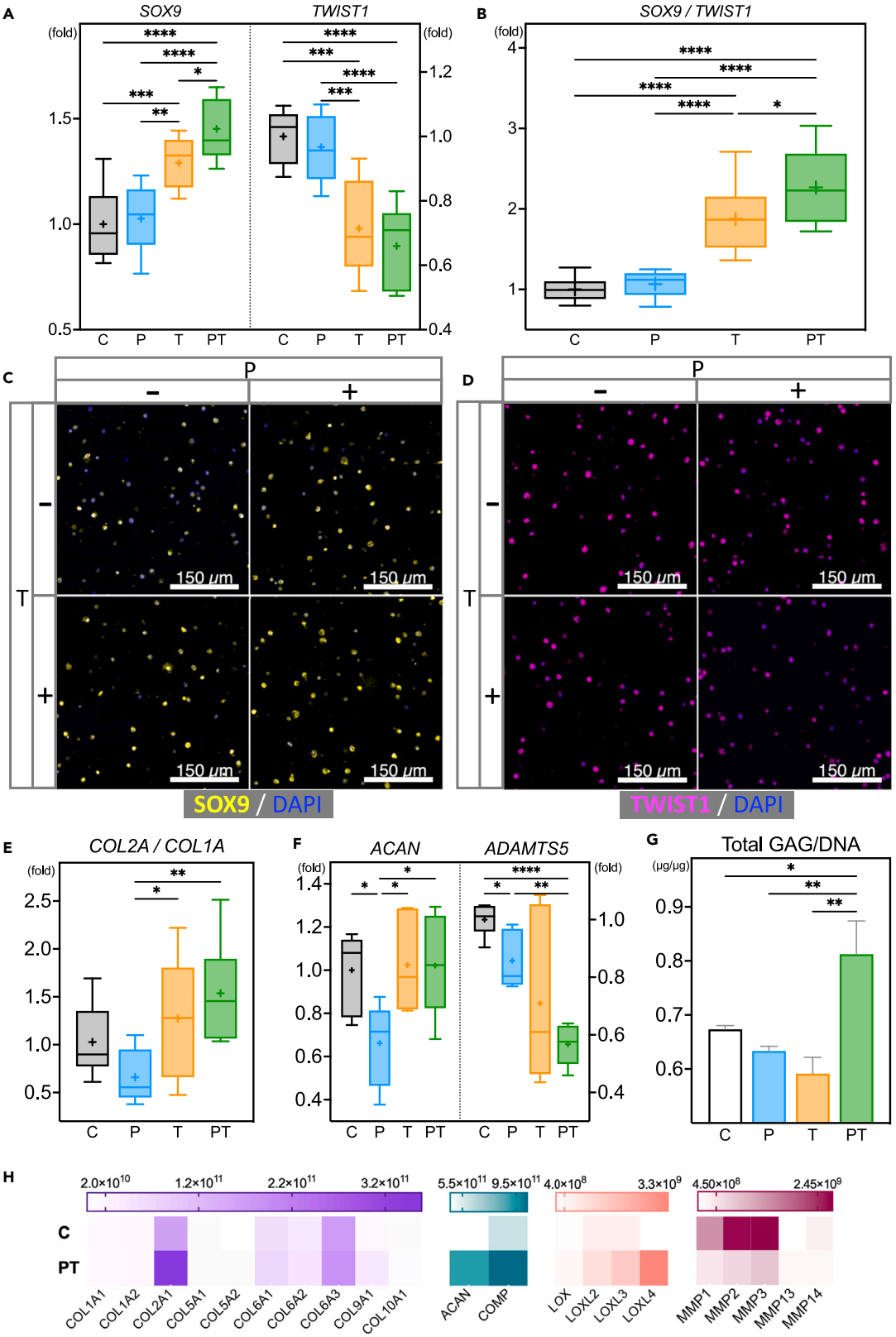
A
SOX9
TWIST1
(fold)
C P T PT
B
SOX9 / TWIST1
C
P
T
PT
150 μm
SOX9 / DAPI
D
TWIST1 / DAPI
E
COL2A / COL1A
F
ACAN
ADAMTS5
G
Total GAG/DNA
(μg/μg)
H
COL1A1 COL1A2 COL2A1 COL5A1 COL5A2 COL6A1 COL6A2 COL6A3 COL9A1 COL10A1
ACAN COMP
LOX LOXL2 LOXL3 LOXL4
MMP1 MMP2 MMP3 MMP13 MMP14

**Figure 4. Chondroinduction response of HP-T stimulation on chondrocytes**

Chondroinduction related gene (n = 6–9) and protein analyses (n = 3–6) for human adult chondrocyte-laden constructs subjected to different stimulations: "C" represents unstimulated control; "P" represents isolated HP stimulation; "T" represents isolated thermal stimulation; "PT" represents combined HP-T stimulation (as described in Figure 2). Relative mRNA expression of (A) *SOX9* and *TWIST1* as well as (B) their ratio. Immunofluorescent staining for (C) SOX9 (D) and TWIST1 protein (DAPI: blue; SOX9: yellow; TWIST1: magenta).

(E) Relative gene expression for *COL2A* versus *COL1A*.

(F) Relative gene expression of aggrecan (*ACAN*) and *ADAMTS5*.

(G) Total GAG quantification normalized to the DNA quantity of the sample.

(H) Heatmap of the LFQ (label-free quantification intensity from mass spectrometry, indicating protein abundance) intensity of various proteins identified by mass spectrometry of the human cartilage explant after 5 days of either free-swelling ("C") or combined stimulation of HP and T ("PT"). Box and whisker plots represent the median, interquartile range, and the minimum and maximum values, with the "+" sign in the boxplots showing the mean. Bar charts show mean and standard error of the mean. Significance is correlated to the p value from Brown-Forsythe and Welch ANOVA tests or one-way ANOVA tests (see STAR Methods section for more details): $p < 0.05$ (*), $p < 0.01$ (**), $p < 0.001$ (***), $p < 0.0001$ (****).

has been investigated, with antioxidant maintenance (e.g., HO-1 and Nrf2) potentially offering protection against OA development.[29] In addition, abnormal mechanical loading regimes have been reported to promote cartilage degradative activities. Mechano-sensing molecules like integrins and ion channels may be responsible for converting external stresses into catabolic events in chondrocytes via mechanotransducive signaling pathways.[30] Yet, more insights from different perspectives are required to establish a fuller picture of the mechanism behind cartilage degeneration and then to possibly restore the function of OA cartilage.

## Cooperative HP-thermal stimulation in cartilage homeostasis

To our knowledge, this research represents the first attempt to scrutinize the collaborative influence of hydrostatic pressure (HP) and biomimetic thermal stimulation—two biophysical cues that are notably diminished in deteriorated cartilage. Using a newly developed bioreactor, we found that the naturally co-occurring HP and thermal signals could enhance each other when applied together in GelMA-based chondrocyte-laden constructs. We observed that biomolecules promoting chondroinduction or chondroprotection, such as SOX9, aggrecan, glycosaminoglycan, *COL2A*, and HSP70, reached their highest levels when the combined stimulation (i.e., HP and biomimetic thermal increase) was applied, compared to isolated stimulations. Conversely, biomolecules with negative effects, such as TWIST1, *ADAMTS5*, *COX2*, and *TNF-a*, exhibited their lowest levels under combined HP-thermal stimulation. This finding supports the idea that chondrocytes may require combined stimulations during daily activities.[31] Specifically, cooperative HP-thermal stimulations could help maintain optimal chondroinductive and chondroprotective responses in chondrocytes, fostering a virtuous cycle in healthy cartilage (Figure 6 top).

Our primary objective is anchored in elucidating the responsive mechanisms of healthy chondrocytes to cyclic hydrostatic pressure and physiological temperature increase. Despite this, we took a preliminary step in extrapolating potential implications in the context of OA. These extrapolations are based on the clearly superior chondroinductive and chondroprotective responses observed under combined HP-T stimulation compared to isolated HP, isolated T, or unstimulated conditions. We suggested that the optimal conditions for chondroinduction and chondroprotection, which are facilitated by HP-T in healthy cartilage, might be unachievable in a degenerative environment where the combined effects of HP-T are diminished or absent (a consequence of altered microstructure[12,13]). Consequently, when chondrocytes are unable to provide optimal chondroinduction and chondroprotection, their capacity to maintain cartilage homeostasis at an ideal level diminishes. This weakened homeostatic support facilitates further degradation of the degenerated cartilage, potentially perpetuating a vicious cycle of deterioration (Figures 1B and 6 bottom). We recognize the potential variability in OA cell behavior compared to the healthy adult chondrocytes we examined. While the heterogeneity of chondrocytes in OA cartilage somewhat supports the generalizability of our findings to the responses of cells present in OA cartilage,[32] our suggested vicious cycle theory still requires confirmation in future studies.

We consistently observed that concomitant application of HP and thermal stimulation resulted in a heightened chondroinductive and chondroprotective response compared to individual stimulations. The synergistic effect of multiple external interventions is not a novel concept in biology. For example, drugs targeting the same cell receptors can occasionally induce signaling pathway crosstalk, leading to cross-tolerance or synergistic effects.[33] We hypothesize that cross-membrane ion channels sensitive to both mechanical and thermal stimuli, such as TRPV4 and TREK1, facilitate signaling crosstalk and an amplified downstream response when HP and thermal stimulation are combined. TRPV4 is an HP and thermally sensitive calcium channel with an activation temperature within the range of our thermal stimulations (32.5°C–38.7°C).[19,20,34] Moreover, TRPV4 has been associated with OA progression and the enhanced chondrogenic response observed in thermal-compressive stimulation.[19,35] The PCR analysis of TRPV4 during HP-T stimulation illustrated that the individual applications of HP and T enhanced the mRNA levels of TRPV4, while their combined stimulation maximized its expression (Figure S6). This supports existing research highlighting TRPV4's role as a sensory calcium channel responsive to variations in hydrostatic pressure and temperature.[19,36–38] Importantly, the observed changes in TRPV4 expression could potentially serve as an indicator that the chondrocytes indeed sensed the distinct biophysical stimulations during our experiment, suggesting a possible role for TRPV4 in the synergistic regulation of chondroinduction and chondroprotection induced by HP-T stimulation. Future in-depth investigations on signaling pathways, such as using specific drugs targeting certain signaling pathways, are warranted to elucidate the mechanism behind the beneficial cooperative effect of HP and thermal stimulation. Unlocking the potential of intermediate regulators in harnessing the combined effects of hydrostatic pressure (HP) and thermal stimulation remains an unexplored avenue in this study. These molecular regulators, which are produced through biophysical stimulations,

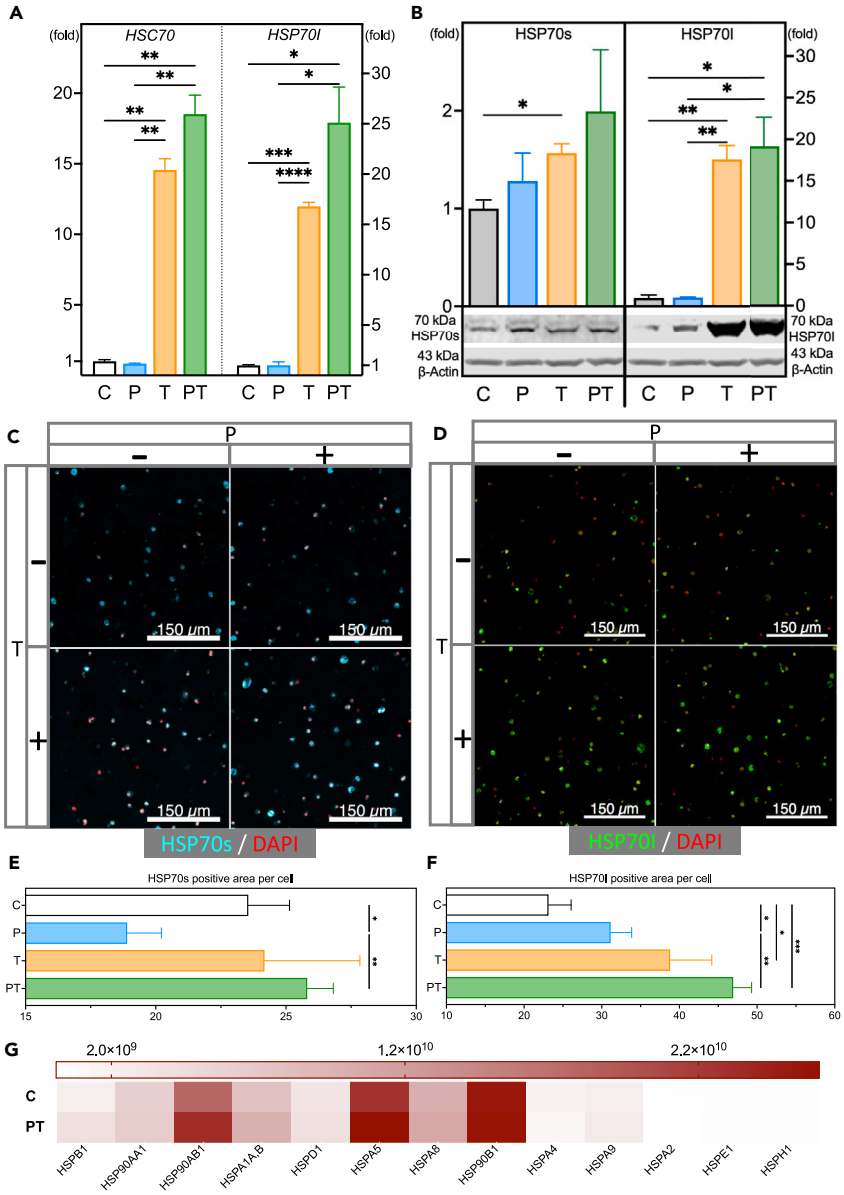


**Figure 5. Chondroprotection response of HP-T stimulation on chondrocytes**

HSP70 gene and protein analyses for human adult chondrocyte-laden constructs subjected to different stimulations: "C" represents unstimulated control; "P" represents isolated HP stimulation; "T" represents isolated thermal stimulation; "PT" represents combined HP-T stimulation (as described in Figure 2) (A-F, n = 3). Relative mRNA expression of (A) *HSC70*, *HSP70I* and (B) Western blot results targeting HSP70 family (HSP70s) and isoform HSP70I. Immunofluorescent staining for (C) HSP70s, shown in cyan, and (D) isoform HSP70I, shown in green. DAPI was shown in red. Image quantification for (E) HSP70s and (F) HSP70I. (G) Heatmap of the LFQ (label-free quantification intensity from mass spectrometry, indicating protein abundance) intensity of various proteins from the HSP family identified by mass spectrometry of the human cartilage explant after 5 days of either free-swelling ("C") or combined stimulation of HP and T ("PT") (HSP70 family were shown as HSPA). Bar charts show mean and standard error of the mean. Significance is correlated to the p value from Brown-Forsythe and Welch ANOVA tests or one-way ANOVA tests (see STAR Methods section for more details): $p < 0.05$ (*), $p < 0.01$ (**), $p < 0.001$ (***), $p < 0.0001$ (****).

hold promise as alternatives to pharmaceutical solutions, potentially achieving similar stimulatory effects in situations where using a bioreactor may be difficult.[39]

## Chondroinduction and chondroprotection

Before subjecting samples to biophysical stimulations in the bioreactor, we labeled key structural proteins with immunofluorescent staining to confirm the maturity of the chondrocytes. This assured us that any observed changes resulted from mature chondrocytes responding to

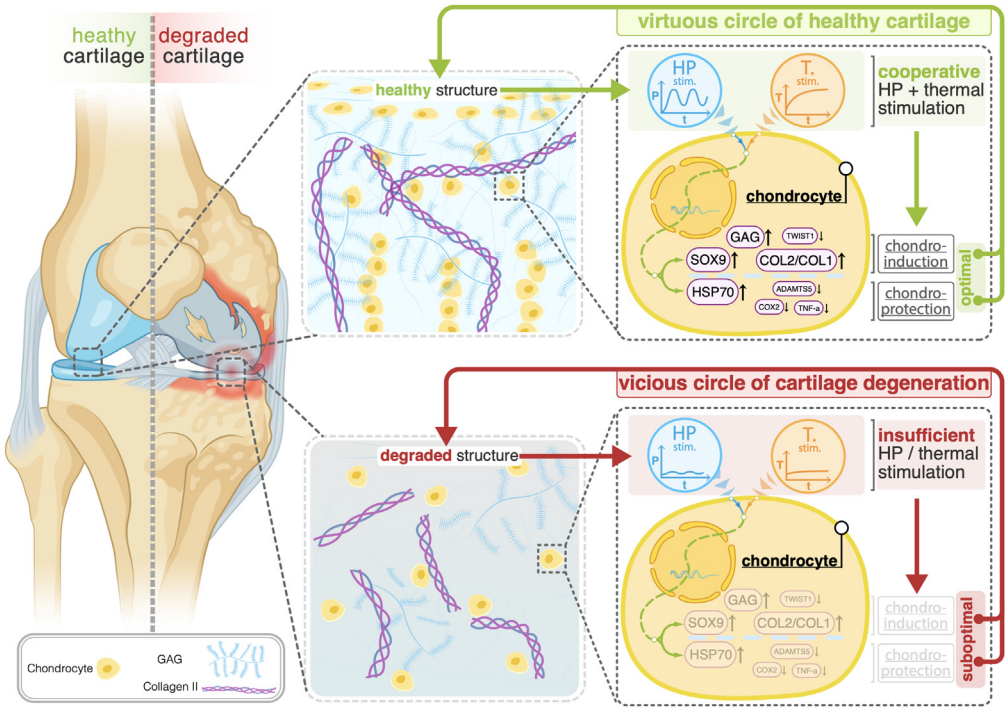


**Figure 6. Proposed mechanism for the regulation of cartilage homeostasis**

Virtuous circle and vicious circle underlying the role of cooperative effect of HP and thermal stimulation in cartilage homeostasis and in cartilage degeneration.

external stimuli, rather than dedifferentiated chondrocytes undergoing redifferentiation (Figure S7). Thermal stimulation alone notably elevated SOX9 (the master gene of chondrogenesis) expression while diminishing TWIST1 (an essential inhibitor of chondrogenesis and SOX9), consistent with our previous work utilizing chondrocyte-seeded HEMA constructs.[19,20] Although biomimetic temperature increases as thermal stimulation remains unexplored outside our group, it is acknowledged that culture temperature can greatly impact chondrocyte metabolism.[17,18] In our experiments, isolated cyclic HP stimulation neither significantly upregulated *SOX9* nor downregulated *TWIST1* gene expression. This outcome may be ascribed to mature chondrocytes' desensitization to mechanical stimuli regarding *SOX9* expression levels following continuous days of stimulation.[40] Given the antagonistic nature between these signaling proteins, the inverse trends observed for *SOX9* and *TWIST1* coincide. We observed that isolated HP stimulation decreased the quantity of aggrecan and s-GAG. This observation is consistent, to some extent, with the research conducted by Savadipour et al. in 2020, in which porcine chondrocytes were encapsulated in agarose hydrogel and the s-GAG level was determined.[38] The s-GAG production of groups subjected to cyclic hydrostatic pressure of 5 MPa at 1 Hz, identical to our loading pattern, was found to be reduced by up to 6-folds. Parkkinnen et al. similarly demonstrated that hydrostatic pressure inhibited s-GAG synthesis in monolayer bovine cell cultures.[41] Other literatures have reported that HP stimulation can also lead to chondrocyte aggrecan upregulation.[16] Nevertheless, this does not contradict our findings that the response of chondrocytes to external HP stimulation is tightly dependent on species (human/animal), cell type (chondrocyte/stem cells), cell culture (monolayer/3D), and loading regimes (amplitude, frequencies, and durations).[38] To ensure that the downregulation was not due to a series of events resulting from lower cell viability, we assessed the viability of the cells using live/dead labeling and found no evidence of increased cell death in the isolated HP loading group (Figure S8). The total amount of DNA per sample (indicative of cell number) was also quantified, and no obvious difference was found across the different stimulation groups (Figure S1). This indicated that the lower s-GAG level in isolated HP and thermal stimulation group is not a consequence of decreased cell viability but it might be attributed to an alteration in cell metabolism, as previously described in the 2020 study by Savadipour et al. Aiming to explore the combined effect of HP and thermal stimulation, we are particularly intrigued by the relationship between the effects produced by isolated and combined stimulations. In this context, the reduced s-GAG level in the HP-isolated group emphasizes the necessity of integrating biomimetic thermal increase with HP stimulation to achieve the most potent chondroinduction response. Furthermore, we postulate that the observed difference between isolated and combined stimulation groups would intensify if experiments were conducted over a more extended period. In conclusion, the cooperative application of HP and thermal stimulation appears to promote chondroinduction in chondrocytes more effectively than either the control or the individual application of these two biophysical stimuli.

HSP70 is a chaperon protein that helps protect cells against a variety of stresses. It has been reported that HSP70 has a beneficial influence on the severity of OA, and its overexpression can suppress apoptosis in osteoarthritic chondrocytes.[21,22,42,43] It was also speculated that in OA, HSP70 level was not sufficient enough to cope with stress-induced damages.[21] In addition, HSP70 is known to be favorably associated

with chondrogenesis. Li et al. have demonstrated that downregulation of HSP70 impairs chondrogenic differentiation in human MSC stem cells.[44] By using HSP70 inhibition assay with quercetin, Tonomura et al. have demonstrated that HSP70 is related to heat shock-induced proteoglycan increase.[21] In our study, thermal stimulations significantly boosted the gene expression of *HSP70*. Notably, HSP70 is commonly upregulated in response to heat-induced stress. However, in our study, the applied thermal stimulation followed a biomimetic temperature increase from 32.5°C to 38.7°C over a duration of 1.5 h. It is important to highlight that this thermal stimulation regime remained well below the threshold considered detrimental to cells, typically exceeding 40°C (which could lead to more cell death). Consequently, the cells subjected to thermal stimulation in our study were able to avoid heat stress conditions (as evidenced by the unchanged cellular viability depicted in Figure S7), while still exhibiting an elevation in HSP70 levels. This increase in HSP70 expression is thought to cf. beneficial effects on chondrocytes, thereby highlighting the favorable impact of the transient thermal stimulation. Even though HP stimulation did not directly impact the *HSP70* gene expression level, it appears to be able to sensitize chondrocytes to the thermal stimulation. We observed a greater increase of *HSP70* gene expression in the combined stimulation group as compared to the thermal stimulation group. In light of our new findings, we can assume that in healthy cartilage, the combined application of HP and thermal stimulations can induce an upregulation of HSP70 in chondrocytes offering an enhanced chondroprotection. In other words, in degenerated cartilage when HP and heat stimulations cannot be maintained during everyday activities, a deficiency of HSP70 can be followed by a cascade of catabolic processes such as abnormal apoptosis.[21,45,46] *ADAMTS5*, an aggrecanase responsible for the degradation of aggrecan in the extracellular matrix of cartilage, has long been implicated in the pathogenesis of OA.[26] The observed downregulation of this enzyme in the combined stimulation group suggests a protective effect on the integrity of the cartilage matrix. Similarly, *COX2* and *TNF-alpha* have been discovered to be related with osteoarthritis, and inhibitors targeting these two proteins have been utilized to treat OA.[25,27] The increased downregulation of these two proteins in the HP thermal stimulation group provides additional support that the combination of HP and thermal stimulation in chondrocytes may provide a more chondroprotective environment, whereas the absence of either HP or thermal stimulation will diminish the chondroprotection effect, resulting in more degenerated cartilage.

### Rationale for biological sample selection

Our primary goal in this study was to explore the impact of hydrostatic pressure and thermal (HP-T) stimulation on chondrocytes. The study naturally gravitated toward a pronounced focus on mature chondrocytes, given the prevalent incidence of cartilage degradation in the adult population. Yet, it was important to our research to also incorporate insights from infant chondrocyte responses to furnish a more comprehensive understanding of chondrocyte behavior across different age groups. By demonstrating a similar trend in the infant chondrocyte responses to HP-T stimuli, we wish to illustrate the universal potential of HP-T synergy in promoting optimum chondroinduction and chondroprotection across different age groups. To provide a more rounded perspective, we further integrated data derived from the cartilage explants of a 14-year-old donor, enhancing the depth of our research. Although incorporating OA cells in our experiment might naturally appear to affirm the vicious cycle theory from a more realistic standpoint, it falls beyond the central scope of the current study. As we progress in this newly explored field of combined HP-T stimulation, we view our current work as establishing a fundamental framework for future research. This initial exploration is designed to encourage more focused research, probing deeper into the complex details of chondrocyte function influenced by HP-T stimulation, potentially extending into *in vivo* experiments in future studies.

### Limitations of the study

(1) This study entailed a comprehensive mid-short-term investigation spanning over two weeks. Although the duration and choice of endpoint analysis may not have allowed for the complete observation of substantial changes in structural protein levels or the tracking of kinetic changes in individual proteins, it successfully captured the cumulative cellular response of chondrocytes to various stimulation regimes over multiple days. The comprehensive nature of our study yielded valuable insights and provided robust evidence to support our hypothesis.

(2) Admittedly, our study is rooted in the exploration of the advantageous impact of synergistic HP-thermal stimulation under optimal conditions. Using our newfound insights, we endeavored to elucidate and extend the comprehension of the vicious cycle of cartilage degeneration. However, to truly substantiate the proposed theory of vicious cycle in a real world, degenerative context, it is imperative to employ OA chondrocytes procured from a diverse range of donors, alongside a more extensive array of biomarkers inherent to an OA condition. Despite these limitations, our study marks a unique investigation of the vicious cycle via a bio-inspired approach, using combined HP-T stimulation in a specially designed bioreactor system. It provides a valuable, evidence-based foundation for further inquiries into cartilage degeneration and its potential treatments.

## STAR★METHODS

Detailed methods are provided in the online version of this paper and include the following:

- KEY RESOURCES TABLE
- RESOURCE AVAILABILITY
  - Lead contact
  - Materials availability

- Data and code availability
- EXPERIMENTAL MODEL AND STUDY PARTICIPANT DETAILS
  - Cell lines
  - Human cartilage explant
- METHOD DETAILS
  - Primary human chondrocyte cell culture
  - Chondrocyte encapsulation and 3D cell culture
  - Human cartilage explant *ex vivo* culture
  - Biophysical stimulations
  - PCR and sulfated glycosaminoglycan analyses
  - Mass spectrometry-based proteomic analyses
  - Immunofluorescent staining and quantification
  - SDS-PAGE and western blotting
- QUANTIFICATION AND STATISTICAL ANALYSIS

## SUPPLEMENTAL INFORMATION

Supplemental information can be found online at https://doi.org/10.1016/j.isci.2023.108519.

## ACKNOWLEDGMENTS

We would like to thank Sandra Jaccoud for her assistance in protocols of biological analyses. We would like to thank EPFL PCF facility for their assistance in proteomic analyses. We would like to thank EPFL ATME workshop for their assistance in manufacturing the parts for the bioreactor. Part of Figure 6 was "created with BioRender.com" with the license for publication. This research is supported by SNF grant # CRSII5_189913.

## AUTHOR CONTRIBUTIONS

Conceptualization: Y.G., T.S., N.N., L.A., and D.P.P.; Methodology: Y.G. and T.S.; Validation: Y.G. and T.S.; Formal Analysis: Y.G., T.S., and N.N.; Investigation: Y.G., T.S., and N.N.; Writing – Original Draft: Y.G., Writing – Review & Editing: Y.G., T.S., N.N., P.K., V.K.R., L.A.L.A, and D.P.P.; Supervision: D.P.P.; Funding Acquisition: D.P.P.

## DECLARATION OF INTERESTS

The authors declare no competing interests.

## INCLUSION AND DIVERSITY

We support inclusive, diverse, and equitable conduct of research.

Received: July 19, 2023
Revised: November 13, 2023
Accepted: November 20, 2023
Published: November 22, 2023

## REFERENCES

1. Goldring, M.B., and Marcu, K.B. (2009). Cartilage homeostasis in health and rheumatic diseases. Arthritis Res. Ther. *11*, 224.
2. Fujii, Y., Liu, L., Yagasaki, L., Inotsume, M., Chiba, T., and Asahara, H. (2022). Cartilage Homeostasis and Osteoarthritis. Int. J. Mol. Sci. *23*, 6316.
3. Hodgkinson, T., Kelly, D.C., Curtin, C.M., and O'Brien, F.J. (2022). Mechanosignalling in cartilage: an emerging target for the treatment of osteoarthritis. Nat. Rev. Rheumatol. *18*, 67–84.
4. Molnar, V., Matišić, V., Kodvanj, I., Bjelica, R., Jeleč, Ž., Hudetz, D., Rod, E., Čukelj, F., Vrdoljak, T., Vidović, D., et al. (2021). Cytokines and Chemokines Involved in Osteoarthritis Pathogenesis. Int. J. Mol. Sci. *22*, 9208.
5. Hwang, H.S., and Kim, H.A. (2015). Chondrocyte Apoptosis in the Pathogenesis of Osteoarthritis. Int. J. Mol. Sci. *16*, 26035–26054.
6. Ansari, M.Y., Ahmad, N., and Haqqi, T.M. (2020). Oxidative stress and inflammation in osteoarthritis pathogenesis: Role of polyphenols. Biomed. Pharmacother. *129*, 110452.
7. Poulet, B., and Beier, F. (2016). Targeting oxidative stress to reduce osteoarthritis. Arthritis Res. Ther. *18*, 32.
8. Blasioli, D.J., and Kaplan, D.L. (2014). The Roles of Catabolic Factors in the Development of Osteoarthritis. Tissue Eng. Part B Rev. *20*, 355–363.
9. Leong, D.J., Hardin, J.A., Cobelli, N.J., and Sun, H.B. (2011). Mechanotransduction and cartilage integrity: Leong et al. Ann. N. Y. Acad. Sci. *1240*, 32–37.
10. Wong, M., and Carter, D.R. (2003). Articular cartilage functional histomorphology and mechanobiology: a research perspective. Bone *33*, 1–13.
11. Abdel-Sayed, P., Vogel, A., Moghadam, M., and Pioletti, D. (2013). Cartilage self-heating contributes to chondrogenic expression. Eur. Cell. Mater. *26*, 171–178.
12. Abdel-Sayed, P., Moghadam, M.N., Salomir, R., Tchernin, D., and Pioletti, D.P. (2014). Intrinsic viscoelasticity increases temperature in knee cartilage under physiological loading. J. Mech. Behav. Biomed. Mater. *30*, 123–130.
13. Setton, L.A., Elliott, D.M., and Mow, V.C. (1999). Altered mechanics of cartilage with osteoarthritis: human osteoarthritis and an

experimental model of joint degeneration. Osteoarthritis Cartilage *7*, 2–14.
14. Becher, C., Springer, J., Feil, S., Cerulli, G., and Paessler, H.H. (2008). Intra-articular temperatures of the knee in sports – An in-vivo study of jogging and alpine skiing. BMC Musculoskelet. Disord. *9*, 46.
15. Martin, J.A., and Buckwalter, J.A. (2001). Roles of articular cartilage aging and chondrocyte senescence in the pathogenesis of osteoarthritis. Iowa Orthop. J. *21*, 1–7.
16. Elder, B.D., and Athanasiou, K.A. (2009). Hydrostatic Pressure in Articular Cartilage Tissue Engineering: From Chondrocytes to Tissue Regeneration. Tissue Eng. Part B Rev. *15*, 43–53.
17. Ito, A., Nagai, M., Tajino, J., Yamaguchi, S., Iijima, H., Zhang, X., Aoyama, T., and Kuroki, H. (2015). Culture Temperature Affects Human Chondrocyte Messenger RNA Expression in Monolayer and Pellet Culture Systems. PLoS One *10*, e0128082.
18. Ito, A., Aoyama, T., Iijima, H., Tajino, J., Nagai, M., Yamaguchi, S., Zhang, X., and Kuroki, H. (2015). Culture temperature affects redifferentiation and cartilaginous extracellular matrix formation in dedifferentiated human chondrocytes: CULTURE TEMPERATURE IN CHONDROCYTES. J. Orthop. Res. *33*, 633–639.
19. Nasrollahzadeh, N., Karami, P., Wang, J., Bagheri, L., Guo, Y., Abdel-Sayed, P., Laurent-Applegate, L., and Pioletti, D.P. (2022). Temperature evolution following joint loading promotes chondrogenesis by synergistic cues via calcium signaling. Elife *11*, e72068.
20. Stampoultzis, T., Guo, Y., Nasrollahzadeh, N., Karami, P., and Pioletti, D.P. (2023). Mimicking Loading-Induced Cartilage Self-Heating *in Vitro* Promotes Matrix Formation in Chondrocyte-Laden Constructs with Different Mechanical Properties. ACS Biomater. Sci. Eng. *9*, 651–661.
21. Tonomura, H., Takahashi, K.A., Mazda, O., Arai, Y., Shin-Ya, M., Inoue, A., Honjo, K., Hojo, T., Imanishi, J., and Kubo, T. (2008). Effects of heat stimulation via microwave applicator on cartilage matrix gene and HSP70 expression in the rabbit knee joint. J. Orthop. Res. *26*, 34–41.
22. Etienne, S., Gaborit, N., Henrionnet, C., Pinzano, A., Galois, L., Netter, P., Gillet, P., and Grossin, L. (2008). Local induction of heat shock protein 70 (Hsp70) by proteasome inhibition confers chondroprotection during surgically induced osteoarthritis in the rat knee. Bio Med. Mater. Eng. *18*, 253–260.
23. Grossin, L., Cournil-Henrionnet, C., Watrin-Pinzano, A., Terlain, B., Jouzeau, J., Netter, P., and Gillet, P. (2003). Overexpression and induction of heat shock protein 70 protect chondrocytes from cell death in vitro and in vivo. Arthritis Res. Ther. *5*, 53.
24. Tonomura, H., Takahashi, K.A., Mazda, O., Arai, Y., Inoue, A., Terauchi, R., Shin-Ya, M., Kishida, T., Imanishi, J., and Kubo, T. (2006). Glutamine protects articular chondrocytes from heat stress and NO-induced apoptosis with HSP70 expression. Osteoarthritis Cartilage *14*, 545–553.
25. Ou, Y., Tan, C., An, H., Jiang, D., Quan, Z., Tang, K., and Luo, X. (2012). Selective COX-2 inhibitor ameliorates osteoarthritis by repressing apoptosis of chondrocyte. Med. Sci. Monit. *18*, BR247–BR252.
26. Jiang, L., Lin, J., Zhao, S., Wu, J., Jin, Y., Yu, L., Wu, N., Wu, Z., Wang, Y., and Lin, M. (2021). ADAMTS5 in Osteoarthritis: Biological Functions, Regulatory Network, and Potential Targeting Therapies. Front. Mol. Biosci. *8*, 703110.
27. Chisari, E., Yaghmour, K.M., and Khan, W.S. (2020). The effects of TNF-alpha inhibition on cartilage: a systematic review of preclinical studies. Osteoarthritis Cartilage *28*, 708–718.
28. Yao, Q., Wu, X., Tao, C., Gong, W., Chen, M., Qu, M., Zhong, Y., He, T., Chen, S., and Xiao, G. (2023). Osteoarthritis: pathogenic signaling pathways and therapeutic targets. Signal Transduct. Target. Ther. *8*, 56.
29. Chen, Z., Zhong, H., Wei, J., Lin, S., Zong, Z., Gong, F., Huang, X., Sun, J., Li, P., Lin, H., et al. (2019). Inhibition of Nrf2/HO-1 signaling leads to increased activation of the NLRP3 inflammasome in osteoarthritis. Arthritis Res. Ther. *21*, 300.
30. Zhao, Z., Li, Y., Wang, M., Zhao, S., Zhao, Z., and Fang, J. (2020). Mechanotransduction pathways in the regulation of cartilage chondrocyte homoeostasis. J. Cell Mol. Med. *24*, 5408–5419.
31. Huang, X., Das, R., Patel, A., and Nguyen, T.D. (2018). Physical Stimulations for Bone and Cartilage Regeneration. Regen. Eng. Transl. Med. *4*, 216–237.
32. Wang, X., Ning, Y., Zhang, P., Poulet, B., Huang, R., Gong, Y., Hu, M., Li, C., Zhou, R., Lammi, M.J., and Guo, X. (2021). Comparison of the major cell populations among osteoarthritis, Kashin–Beck disease and healthy chondrocytes by single-cell RNA-seq analysis. Cell Death Dis. *12*, 551.
33. Dumas, E.O., and Pollack, G.M. (2008). Opioid Tolerance Development: A Pharmacokinetic/Pharmacodynamic Perspective. AAPS J. *10*, 537–551.
34. O'Conor, C.J., Leddy, H.A., Benefield, H.C., Liedtke, W.B., and Guilak, F. (2014). TRPV4-mediated mechanotransduction regulates the metabolic response of chondrocytes to dynamic loading. Proc. Natl. Acad. Sci. USA *111*, 1316–1321.
35. McNulty, A.L., Leddy, H.A., Liedtke, W., and Guilak, F. (2015). TRPV4 as a therapeutic target for joint diseases. Naunyn-Schmiedeberg's Arch. Pharmacol. *388*, 437–450.
36. Pattappa, G., Zellner, J., Johnstone, B., Docheva, D., and Angele, P. (2019). Cells under pressure – the relationship between hydrostatic pressure and mesenchymal stem cell chondrogenesis. Eur. Cell. Mater. *37*, 360–381.
37. Güler, A.D., Lee, H., Iida, T., Shimizu, I., Tominaga, M., and Caterina, M. (2002). Heat-Evoked Activation of the Ion Channel, TRPV4. J. Neurosci. *22*, 6408–6414.
38. Savadipour, A., Nims, R.J., Katz, D.B., and Guilak, F. (2022). Regulation of chondrocyte biosynthetic activity by dynamic hydrostatic pressure: the role of TRP channels. Connect. Tissue Res. *63*, 69–81.
39. Otarola, G.A., Hu, J.C., and Athanasiou, K.A. (2022). Ion modulatory treatments toward functional self-assembled neocartilage. Acta Biomater. *153*, 85–96.
40. Bleuel, J., Zaucke, F., Brüggemann, G.P., and Niehoff, A. (2015). Effects of Cyclic Tensile Strain on Chondrocyte Metabolism: A Systematic Review. PLoS One *10*, e0119816.
41. Parkkinen, J.J., Ikonen, J., Lammi, M.J., Laakkonen, J., Tammi, M., and Helminen, H.J. (1993). Effects of Cyclic Hydrostatic Pressure on Proteoglycan Synthesis in Cultured Chondrocytes and Articular Cartilage Explants. Arch. Biochem. Biophys. *300*, 458–465.
42. Kubo, T., Arai, Y., Takahashi, K., Ikeda, T., Ohashi, S., Kitajima, I., Mazda, O., Takigawa, M., Imanishi, J., and Hirasawa, Y. (2001). Expression of Transduced HSP70 Gene Protects Chondrocytes from Stress. J. Rheumatol. *28*, 330–335.
43. Zhang, C., Sanghvi, A., Kirsch, T., Raya, J.G., and Ruiz, A. (2022). LEVERAGING HSP70 TO PROTECT CHONDROCYTES FROM APOPTOSIS PROGRESSION AFTER JOINT INJURY. Osteoarthritis Cartilage *30*, S244–S245.
44. Li, C., Sunderic, K., Nicoll, S.B., and Wang, S. (2018). Downregulation of Heat Shock Protein 70 Impairs Osteogenic and Chondrogenic Differentiation in Human Mesenchymal Stem Cells. Sci. Rep. *8*, 553.
45. Rérole, A.-L., Jego, G., and Garrido, C. (2011). Hsp70: Anti-apoptotic and Tumorigenic Protein. In Molecular Chaperones Methods in Molecular Biology, S.K. Calderwood and T.L. Prince, eds. (Humana Press), pp. 205–230.
46. Lee, J.-S., Lee, J.-J., and Seo, J.-S. (2005). HSP70 Deficiency Results in Activation of c-Jun N-terminal Kinase, Extracellular Signal-regulated Kinase, and Caspase-3 in Hyperosmolarity-induced Apoptosis. J. Biol. Chem. *280*, 6634–6641.
47. Karami, P., Nasrollahzadeh, N., Wyss, C., O'Sullivan, A., Broome, M., Procter, P., Bourban, P.E., Moser, C., and Pioletti, D.P. (2021). An Intrinsically-Adhesive Family of Injectable and Photo-Curable Hydrogels with Functional Physicochemical Performance for Regenerative Medicine. Macromol. Rapid Commun. *42*, 2000660.
48. Karami, P., Wyss, C.S., Khoushabi, A., Schmocker, A., Broome, M., Moser, C., Bourban, P.-E., and Pioletti, D.P. (2018). Composite Double-Network Hydrogels To Improve Adhesion on Biological Surfaces. ACS Appl. Mater. Interfaces *10*, 38692–38699.

## STAR★METHODS

### KEY RESOURCES TABLE

| REAGENT or RESOURCE | SOURCE | IDENTIFIER |
|---|---|---|
| Antibodies | | |
| Mouse anti-SOX9 | Abcam | ab76997 |
| Mouse anti-COL2A | Invitrogen | MA5-12789 |
| Mouse anti-ACAN | Invitrogen | AHP0022 |
| Rabbit anti-TRPV4 | Abcam | Ab191580 |
| Alexa Fluor 568 phalloidin | Invitrogen | A12380 |
| Mouse anti-TWIST1 | Invitrogen | MA5-17195 |
| Mouse anti-HSP70 | Abcam | ab2787 |
| Rabbit anti-HSPA1A | Invitrogen | # PA5-34772 |
| IRDye® 680RD Donkey anti-Mouse | Licor | 926-68072 |
| IRDye® 800CW Donkey anti-Rabbit | Licor | 926-32213 |
| Alexa Fluor 488 anti-Mouse | Invitrogen | A11029 |
| Alexa Fluor 488 anti-Rabbit | Invitrogen | A-21206 |
| Experimental models: Cell lines | | |
| Healthy primary human chondrocytes, Caucasian male adult donor | INNOPROT, Spain | #cat 0018996 P10970 |
| Healthy primary human chondrocytes, Caucasian (normally Caucasian as there was the color of white skin on the tissue) male juvenile donor | UTR, CHUV, Switzerland | MF280420 |
| Explant from the knee cartilage, male adolescent donor (from south Africa) | CHUV, Switzerland | / |
| Oligonucleotides | | |
| Primers for PCR | This paper, Microsynth (Balgach, Switzerland) | See supplemental information |
| Software and algorithms | | |
| GraphPad Prism 9 | GraphPad | GraphPad |
| R | R | Details see supplemental information |

### RESOURCE AVAILABILITY

#### Lead contact

Further information and requests for resources and reagents should be directed to and will be fulfilled by the Lead contact, Dominique Pioletti (dominique.pioletti@epfl.ch).

#### Materials availability

This study did not generate unique reagents.

#### Data and code availability

- All data reported in this paper will be shared by the lead contact upon request.
- This paper does not report original code.
- Any additional information required to reanalyze the data reported in this paper is available from the lead contact upon request.

### EXPERIMENTAL MODEL AND STUDY PARTICIPANT DETAILS

#### Cell lines

Two cell sources are used in this study. Primary human chondrocytes were obtained from a healthy 22-year-old male's knee cartilage (P10970, Innoprot, Spain) and served as our primary cell source. Additionally, some experiments were replicated using primary chondrocytes derived

from the distal joint cartilage of an extra finger of a 3.5-day-old male (MF280420-cart, established within GMP standard in UTR at CHUV by Prof Lee Ann Laurent-Applegate). Both cell sources were expanded till passage 4 with medium that was selected based on the suggestions of the cell suppliers. Culture medium was refreshed every three days. Cells were finally trypsinized and collected using trypsin/EDTA (Sigma, US).

### Human cartilage explant

An intra-articular cartilage fragment was obtained from a 14-yo patient. The specimen was obtained from an osteochondritis lesion at the level of the left knee with no known associated inflammatory condition. The clinical cartilage sample was anonymized, stored, and logged in a Musculoskeletal Department Biobank, complying with internal regulations thereof and following an approved protocol (i.e., Vaud cantonal State Ethics Committee reference N°264/12). After washing, the samples were extracted using 5mm biopsy punches and promptly placed into DMEM (ThermoFisher, US) supplemented with 1% L-Glutamine (Gibco, US) and 1% penicillin-streptomycin (P/S) (ThermoFisher, US).

## METHOD DETAILS

### Primary human chondrocyte cell culture

Two cell sources are used in this study. Primary human chondrocytes were obtained from a healthy 22-year-old male's knee cartilage (P10970, Innoprot, Spain) and served as our primary cell source. Additionally, some experiments were replicated using primary chondrocytes derived from the distal joint cartilage of an extra finger of a 3.5-day-old male (MF280420-cart, established within GMP standard in UTR at CHUV by Prof Lee Ann Laurent-Applegate). Both cell sources were expanded till passage 4 with medium that was selected based on the suggestions of the cell suppliers.

Proliferation medium for P10970: minimum essential medium (αMEM) (ThermoFisher, US) supplemented with 10% fetal bovine serum (FBS) (Sigma, US), 1% L-Glutamine (Gibco, US), 1% penicillin-streptomycin (P/S) (ThermoFisher, US), 10mM HEPES buffer (Gibco, US), 10 mM nonessential amino acids (NEEA) (Gibco, US), 1 ng/ml transforming growth factor beta 1 (TGF-β1) (Gibco, US), and 5 ng/ml fibroblast growth factor (FGF2) (Gibco, US).

Proliferation medium for MF280420: DMEM (ThermoFisher, US) supplemented with 10% FBS, 1% L-Glutamine and 1% P/S.

Culture medium was refreshed every three days. Cells were finally trypsinized and collected using trypsin/EDTA (Sigma, US).

### Chondrocyte encapsulation and 3D cell culture

Lyophilized GelMA polymer was synthesized as previously described and then was dissolved in phosphate buffered saline (PBS) (ThermoFisher, US) at 10 wt.%.[47] Photoinitiator LAP (Lithium-Phenyl-2,4,6- trimethylbenzoylphosphinat) (Tocris, UK) was added into the solution with a final concentration of 0.1 mg/ml. Passage 4 human chondrocytes were resuspended in the previous mix at 10 million cells/ml. The cell suspension was then injected in a customized Teflon mold (cylindrical shape, 5 mm diameter, 3 mm thickness) before crosslinking with illumination under 405 nm-wavelength light for two minutes. The hydrogel network was formed through covalent bonding between the methacrylate groups (C=C double bonds) during photopolymerization.[48] The cylindrical chondrocyte laden GelMA constructs were then incubated in cell culture proliferation medium during preincubation period for a week.

### Human cartilage explant *ex vivo* culture

An intra-articular cartilage fragment was obtained from a 14-yo patient. The specimen was obtained from an osteochondritis lesion at the level of the left knee with no known associated inflammatory condition. The clinical cartilage sample was anonymized, stored, and logged in a Musculoskeletal Department Biobank, complying with internal regulations thereof and following an approved protocol (i.e., Vaud cantonal State Ethics Committee reference N°264/12). After washing, the samples were extracted using 5mm biopsy punches and promptly placed into DMEM (ThermoFisher, US) supplemented with 1% L-Glutamine (Gibco, US) and 1% penicillin-streptomycin (P/S) (ThermoFisher, US).

### Biophysical stimulations

After preincubation, the 3D cell-laden constructs were transferred from multi-well plates into the bioreactor loading chambers. The samples were then cultured with a serum-free stimulation medium which consisted of αMEM, 1% P/S, 1% L-Glu, 10 mM HEPES buffer, 10 mM NEAA, 10% insulin transferrin selenium (ITS-IV) (PAN-biotech, Germany), and 1% ascorbic acid (Sigma, US). Samples were stimulated for five consecutive days and the medium inside the chamber was changed every other day. A 1.5-hour stimulation session was conducted on each stimulation day. Four different stimulation groups were conducted in the bioreactor: 1) "C": free swelling (FS) control, incubated at 32.5°C; 2) "P": sinusoidal cyclic hydrostatic pressure loading (5 MPa at 1 Hz), performed at 32.5°C; 3) "T": thermal stimulation where samples were subjected to a gradually increased temperature from 32.5°C to 38.7°C following an evolution curve identical to the temperature increase observed in the knee during physiological loading[19]; 4) "P+T": simultaneous combination of hydrostatic pressure loading and thermal stimulations. Samples were immediately collected for analyses after the last round of the corresponding stimulation. An experimental workflow is presented in Figure 2. For human cartilage explants, the stimulation process began on the second day after receiving them from the hospital and continued for five consecutive days, following the same stimulation protocol used for the cell-laden hydrogels.

### PCR and sulfated glycosaminoglycan analyses

Cell laden GelMA constructs were collected and homogenized in TRIzol (ThermoFisher, US) before chloroform was added into the mix. After centrifugation, the aqua-phase containing total mRNA was extracted and purified with Nucleospin® RNA XS kit (Macherey-Nagel, Germany) following the manufacturer's instructions. Concentration of mRNA was determined using a Nanodrop Lite Spectrophotometer (Thermo Scientific, US), with the A260/A280 ratio around 2.0 confirming high-quality RNA suitable for subsequent PCR reactions. Additionally, an overall RIN value of 9.8 confirmed the efficacy of the RNA extraction methods. Quantitative real-time polymerase chain reaction (RT-qPCR) was performed to quantify the relative gene expression using Taqman® Reverse Transcription Reagents (Applied Biosystems, US) and Fast SYBR® Green PCR Master Mix (Applied Biosystems, US) according to the instructions from the manufacturers. The quantification analysis was performed using ΔΔCt method with the gene of ribosomal protein L13a (*RPL13*) being the endogenous control. All relevant primers were synthesized by Microsynth (Balgach, Switzerland) and their sequences can be seen in supplemental information (Table S1).

To measure the concentration of sulfated glycosaminoglycan (s-GAG) inside the cell laden GelMA construct or in the medium, samples were firstly digested in papain solution (pH = 6.5) containing 6 μl/ml papain enzyme (Sigma, US), 100 mM Na2HPO4, 10 mM L-cysteine, and 10 mM EDTA overnight at 65°C. Next, after centrifugation, the supernatant was extracted, and the s-GAG concentration was quantified by 1,9-dimethylmethylene blue (DMMB, pH = 1.5) dual colorimetric assay. Standard curve was performed with bovine chondroitin sulphate (Sigma, US). The absorbance at 530 nm and 590 nm were examined. DNA concentration was determined using Hoechst 33258 dye (ThermoFisher, US) with calf thymus DNA (ThermoFisher, US) serving as standard. The absorbance and fluorescent signal were measured using a Wallac plate reader.

### Mass spectrometry-based proteomic analyses

Mass spectrometry-based proteomics-related experiments were performed by the Proteomics Core Facility at EPFL. Human explants were homogenized in liquid nitrogen before digestion in RIPA solution. Protein samples underwent short migration on an SDS-PAGE gel to remove the RIPA buffer. Sections containing proteins were excised. Proteins were extracted from the gel then processed for reduction, alkylation, and overnight Trypsin gold digestion. Reconstituted samples underwent nano-flow separations on a Dionex Ultimate 3000 RSLC nano UPLC system, coupled with a QExactive Orbitrap Mass Spectrometer. The 12 most intense ions were selected for high-energy collisional dissociation. Data was processed using MaxQuant 1.6.10.43 against the human Swissprot database. Fixed and variable modifications were set, with a 0.01 FDR cutoff for peptides and proteins. Label-free quantification and normalization were performed using the MaxLFQ algorithm. Further visualizations were created using R scripts.

### Immunofluorescent staining and quantification

Cell laden GelMA constructs were fixed with 4% PAF, frozen in O.C.T. (Tissue-Tek, US), and sectioned with a cryostat (Leica, Germany) at 7 μm. The sections were permeabilized and blocked with 0.25% Triton-X PBS solution and 1% BSA PBS solution before incubation in primary antibody solution at 4°C overnight. Information of all antibodies used in this study can be seen in supplemental information (Table S2). After three washes with PBS, the slides were incubated in FITC-conjugated donkey anti-mouse secondary antibody solution at room temperature for 40 mins followed by DAPI staining and three times washing with PBS to remove excessive dye. The slides were mounted and sealed with Fluoromount-G mounting solution (ThermoFisher, US). Slides were imaged using tile scan under a fluorescent slide scanner (Olympus VS120 whole slide scanner, Japan) with a constant exposure setting applied for all the slides.

Bio-format images from tile scan were stitched and quantified using QuPath software (GitHub, US). For image quantification of signaling proteins such as SOX9 and TWIST1, a consistent threshold was first set for all groups to determine the positive signal in an image. A region of interest (ROI) was delineated to outline the regions that are representative in each sample. Areas exhibiting folds, cracks, and edges were excluded from the ROI to avoid artifacts introduced through cryosectioning and staining procedures. Then the DAPI channel was isolated and used for cell detection within the ROI. Subsequently, all detected cells were classified as either positively or negatively stained for the target molecules based on the predefined threshold. The percentage of positively stained cells was then calculated. For other potentially secretory proteins such as HSP70 and the aggrecan core protein ACAN, the total positive signal intensity was measured based on the predefined threshold and normalized to the number of cells in the region of interest.

### SDS-PAGE and western blotting

Chondrocyte-laden GelMA constructs were lysed in RIPA buffer (Millipore, US) with proteinase and phosphatase inhibitor (Thermal Scientific, US). Protein extraction was quantified using Pierce BCA Protein Assay Kit (Thermo Scientific, US). Extracts were mixed with LDS sample loading buffer (Invitrogen, US) and NuPAGE sample reducing agent (Invitrogen, US), denatured at 95°C for 5 mins, electrophoresed with NuPAGE 4–12% Bis-Tris Gel (Invitrogen) with around 15 mg of total protein per lane, and transferred to a PVDF membrane (Invitrogen, US). Total protein staining was done using Revert700 (Licor, UK) and visualized with Odyssey machine (Licor, US). Membranes were cut, blocked with 5% fat-free milk in PBS-Tween (Sigma, US) and incubated with mouse anti-human HSP-70 antibody (1:250, ab2787, Abcam, UK) and mouse anti-β-actin antibody (1:200, A2228, Sigma, US) at 4°C overnight. Membranes were then washed and incubated with IRDye 680RD secondary antibody (1:5000, Licor, UK) for 2 hours. After washing, membranes were imaged with Odyssey and protein was quantified and normalized using Image Studio (Licor, UK).

## QUANTIFICATION AND STATISTICAL ANALYSIS

Statistical analyses were conducted using GraphPad Prism 9 (GraphPad, US). To compare the results derived from PCR immunoblotting and immunostaining quantifications, we employed Brown-Forsythe and Welch ANOVA tests followed by unpaired t-tests with Welch's correction, with individual variances computed for each comparison. We opted for this methodology due to the inherent variability in gene responses to distinct stimulations. Regarding results involving ratios, such as gene ratios and GAG/DNA quantities, we chose to utilize ordinary one-way ANOVA followed by uncorrected Fischer's LSD test with a single pooled variance for these analyses. Sample sizes can be found in the caption of each result figure. Significance is correlated to the p value: $p < 0.05$ (*), $p < 0.01$ (**), $p < 0.001$ (***), $p < 0.0001$ (****), not significant (ns).